

# Addition in Four Movements: Mapping Layer-wise Information Trajectories in LLMs

Yao Yan

College of Computer and Information Science

Chongqing Normal University

Chongqing Key Lab of Cognitive Intelligence and Intelligent Finance

yaoyan@stu.cqnu.edu.cn

## Abstract

Multi-digit addition is a clear probe of the computational power of large language models. To dissect the internal arithmetic processes in LLaMA-3-8B-Instruct, we combine linear probing with logit-lens inspection. Inspired by the step-by-step manner in which humans perform addition, we propose and analyze a coherent four-stage trajectory in the forward pass: Formula-structure representations become linearly decodable first, while the answer token is still far down the candidate list. Core computational features then emerge prominently. At deeper activation layers, numerical abstractions of the result become clearer, enabling near-perfect detection and decoding of the individual digits in the sum. Near the output, the model organizes and generates the final content, with the correct token reliably occupying the top rank. This trajectory suggests a hierarchical process that favors internal computation over rote memorization. We release our code and data to facilitate reproducibility.

## 1 Introduction

Arithmetic tasks like multi-digit addition have emerged as an important testbed for evaluating whether large language models (LLMs) truly learn generalizable reasoning procedures or simply memorize patterns from their training data (Nikankin et al., 2024). Multi-digit addition is trivial for humans due to a well-defined algorithm (carry propagation), but for an LLM it requires either faithfully emulating that algorithm or finding alternate shortcuts. A model that can correctly add arbitrary numbers is likely executing some internal computation akin to the human algorithm, whereas systematic errors or context-specific failures could imply reliance on superficial heuristics or memorized exemplars.

Prior studies probing LLM arithmetic reveal contrasting hypotheses. One line of work suggests

LLMs develop structured, algorithm-like procedures. For example, analyses of GPT-style models show component specialization for subtasks like partial summation and carry handling, indicative of internal step-by-step solutions (Yu and Ananiadou, 2024). Furthermore, even the minimal two-layer encoder-only Transformer can explicitly learn the human carry-add procedure (e.g., column summation and carry management across layers) (Kruthoff, 2024).

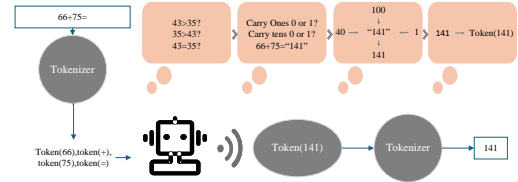


Figure 1: Schematic diagram of the multi-stage information processing model as LLMs solve addition problems. It illustrates how internal representations within the model, characterized by different properties—ranging from understanding problem structure (e.g., formulaic patterns), to core computations (e.g., carries and summations), then to the numerical abstraction of results (e.g., specific digits), and finally to the organization and generation of output—are sequentially activated and detected at different network depths.

However, another line of research argues that LLMs achieve addition largely via simple pattern-matching heuristics rather than robust algorithms (Nikankin et al., 2024). For instance, neuron activation studies suggest models use a “bag of heuristics”—sparsely encoded, pattern-specific strategies (Zhou et al., 2024). This view is supported by findings of generalization failures in large LLMs on out-of-distribution elementary addition; models adept at standard addition performed poorly with unfamiliar symbols or violated commutativity ( $A+B$  vs.  $B+A$ ) (Yan et al., 2025). Such failures imply reliance on surface patterns over learned core addition rules. Complementary evidence indicates pre-

trained LLMs may also leverage latent Fourier representations for addition, combining low-frequency (magnitude) and high-frequency (e.g., parity) features (Zhou et al., 2024).

Thus, a key question arises: when mainstream open-source large language models like LLaMA-3-8B-Instruct (Grattafiori et al., 2024) perform multi-digit addition, is their internal process closer to a human-like step-by-step algorithm (e.g., digit-wise summation with carries), or does it rely on a complex, non-algorithmic pattern extraction mechanism?

To answer this question, we explored the multi-digit addition mechanism of LLaMA-3-8B-Instruct. Our research revealed a clear pattern of evolution in information representation with increasing model depth. Using probing techniques, we observed that information related to different aspects of the addition task became significantly decodable at different layers of the model. This evolutionary pattern can be roughly characterized by the order in which the following information types appear:

1. Formula structure representation (structural understanding and representation of input formula),
2. Emergence of core computational features (representation of key information related to addition operations and carry propagation),
3. Numerical abstraction of results (intermediate computational results are integrated into internal abstract numerical representations),
4. Organization and generation of output content (generation of final answer token and representation of display format).

This observed layering of information representation at different depths suggests that the model uses a structured information processing approach to solve arithmetic tasks, which supports the 'computation rather than memory' hypothesis. Although this is not directly equivalent to the model accurately executing a human-defined algorithm, it reveals an internal processing process that is more complex than simple pattern matching or memory retrieval.

## 2 Related Work

LLMs face the long-standing question of whether their arithmetic competence derives from algorithmic computation or heuristic pattern matching.

Prior work clusters into two camps, with a third line exploring abstract numerical structure.

**Algorithmic evidence.** Fully reverse-engineered toy Transformers show that attention layers can implement a discrete Fourier Transform-style algorithm for modular addition (Nanda et al., 2023); this concept of trigonometric manipulation has been extended to general addition in mid-sized LLMs, which are proposed to use a "Clock" algorithm operating on helical number representations (Kantamneni and Tegmark, 2025). In larger models, component specialization persists: carry-routing heads emerge in 7B GPTs (Yu and Ananiadou, 2024), and layer-wise decomposition into column summation and carry propagation is observed in 7B LLaMA variants (Kruthoff, 2024). Causal mediation pinpoints operand routers and parallel digit streams (Stolfo et al., 2023; Quirke and Barez, 2024).

**Heuristic evidence.** An opposing view holds that correct answers arise from a "bag of heuristics". Neuron-level analyses identify sparse units encoding template-based strategies (Nikankin et al., 2024), while out-of-distribution tests reveal systematic failures when digits are permuted or replaced with novel symbols (Yan et al., 2025).

**Abstract numerical representations.** Beyond this dichotomy, several studies report representations that generalize across operations. Pre-trained LLMs appear to superimpose low-frequency magnitude and high-frequency parity features in a Fourier-like basis (Zhou et al., 2024). Recent work further shows that the *value* of digits is recoverable by a simple linear probe, demonstrating that numbers lie in a low-dimensional linear subspace of hidden states (Zhu et al., 2025). Group-structured arithmetic tasks elicit basis vectors reminiscent of representation theory (Chughtai et al., 2023), and tree-structured reasoning traces have been reconstructed from hidden states (Hou et al., 2023). Complementary evidence shows that LLMs also encode numbers *digit-by-digit*: (Levy and Geva, 2025) identify separate neuron groups for each decimal position and explain typical single-digit mistakes by this representation.

**Our position.** We connect these threads by offering a layer-resolved account of multi-digit addition in LLaMA-3-8B. Combining linear probes (Belinkov, 2022) and the logit lens (nostalgebraist, 2020), we uncover a four-stage

trajectory—from formula recognition to explicit token generation—that reconciles component specialization with the emergence of reusable numerical abstractions.

### 3 Methodology

This study aims to explore the internal information processing flow of the LLaMA3 8B Instruct when performing arithmetic operations (focusing on addition). Our approach uses LLaMA3-8B-Instruct as a base model, explores its internal representation to reveal its mechanism for processing arithmetic problems, and then designs diagnostic probe experiments to test whether the model is calculating the results or just memorizing them. While LLaMA3-8B-Instruct serves as our primary experimental model, we also conducted similar experiments on the Mistral-7B-Instruct(Jiang et al., 2023), Qwen2.5-7B-Instruct(Hui et al., 2024) models and Qwen3-8B(Yang et al., 2025). To maintain the conciseness of the main paper, the corresponding experimental results for these additional models are presented in the appendix D.

#### 3.1 Logit Lens

As a supplementary method, the logit lens technique is employed to observe the model’s evolving predictions. Given a hidden state  $H^{(l)}$  at layer  $l$  (representing the model’s state just before generating the first answer token) and the model’s unembedding matrix  $W_U$ , the logit lens calculates layer-specific output logits  $L^{(l)}$  as:

$$L^{(l)} = H^{(l)} W_U^T$$

These logits  $L^{(l)}$  represent the vocabulary distribution from which the model would predict the next token if layer  $l$  were the final layer. This allows for tracking the layer-wise refinement of the prediction for the initial token of the arithmetic operation’s result.

#### 3.2 Model Architecture and Target Activations

We believe that the foundation for investigating how large language models perform arithmetic operations lies in their ability to correctly solve such problems in the first place. A model that cannot reliably produce accurate arithmetic results would be an unsuitable subject for an in-depth study of its internal computational mechanisms. Therefore, we conducted a preliminary evaluation of

Model	ADD Accuracy
LLAMA3-8B-INSTRUCT	<b>97.29%</b>
Mistral-7B-Instruct	84.99%
Qwen3-8B	83.39%
Qwen2.5-7B-Instruct	60.61%

Table 1: An evaluation of overall accuracy on 1-digit to 6-digit addition tasks among selected open-source LLMs indicated that LLAMA-3-8B-INSTRUCT achieved the highest performance. This superior result formed the basis for its selection, with comprehensive supporting data presented in Appendix A.

arithmetic proficiency across several contemporary open-source large language models. As shown in Table 1, LLAMA-3-8B-INSTRUCT demonstrated the highest accuracy among the evaluated models. This superior performance in correctly answering arithmetic questions established it as the most suitable candidate for this research, providing a solid basis for exploring its internal processing pathways for addition.

Arithmetic tasks are presented to the LLAMA3-8B-INSTRUCT model using a standardized prompt format, e.g., "Calculate: num1+num2 = ". The prompt—including the trailing space character ( $x_S$ ) after the equals sign—is tokenized as  $X = (x_1, x_2, \dots, x_S)$ . The model follows the standard Transformer architecture. At each layer  $l \in \{0, \dots, L-1\}$ , the hidden states from the previous layer  $\mathbf{H}^{(l-1)}$  are updated through self-attention and feed-forward blocks, denoted collectively as  $\mathcal{G}^{(l)}$ :

$$\mathbf{H}^{(l)} = \mathbf{H}^{(l-1)} + \mathcal{G}^{(l)}(\mathbf{H}^{(l-1)}).$$

The initial activations  $\mathbf{H}^{(0)}$  are the sum of token embeddings and positional encodings. For probing, we focus on the hidden vector of the last input token,  $\mathbf{h}_S^{(l)} \in \mathbb{R}^d$ , which is responsible for predicting the first answer token.

#### 3.3 Linear Probe Design, Training, and Evaluation

To determine where arithmetic information (e.g., carries, result digits) is linearly accessible, we train a separate linear probe for each layer  $l$ . Each probe is a logistic classifier that receives  $\mathbf{h}_S^{(l)}$  and produces  $K$  logits:

$$\mathbf{o}^{(l)} = W^{(l)} \mathbf{h}_S^{(l)} + b^{(l)}, \quad W^{(l)} \in \mathbb{R}^{K \times d}, \quad b^{(l)} \in \mathbb{R}^K.$$

A softmax layer converts  $\mathbf{o}^{(l)}$  to class probabilities  $\hat{\mathbf{p}}^{(l)}$ , and the predicted label is  $\hat{y} = \arg \max_k \hat{p}_k^{(l)}$ .

Parameters are optimized with the cross-entropy loss

$$\mathcal{J}(W^{(l)}, b^{(l)}) = -\frac{1}{N} \sum_{i=1}^N \sum_{k=1}^K y_{i,k} \log \hat{p}_{i,k}^{(l)},$$

. Accuracy on a held-out test set reveals how each layer encodes the probed attribute.

### 3.4 Data Handling and Evaluation Criteria

To ensure the rigor of the research and the reliability of the results, this study carefully designed the data processing process and evaluation criteria, which are described in detail as follows:

**Dataset Construction:** All datasets used for training and testing linear probes were custom-built and annotated in this study to target specific information.

**Probe Training and Testing:** For each probing task, linear probes are trained for 10 epochs on a dedicated training set and evaluated on a strictly separate, unseen held-out test set.

**Representation Identification and Characterization of Information Emergence:** When a linear probe achieves a classification accuracy at or near 100% on the corresponding test set, we consider that the model has formed a clear and stable representation of the probed information at that specific layer. This serves as an indicator for locating the critical layer(s) where specific information becomes salient. Subsequently, we analyze the sequential order in which different types of information representations emerge with high decodability across layers to characterize the evolutionary pattern of information processing. All analyses involve layer-wise probing to track the dynamic evolution of information representations across the model’s depth.

## 4 Experiments and Results

We conducted a series of experiments to diagnose how arithmetic features are represented within the LLaMA3-8B-Instruct model. Across all experiments, diagnostic probes were trained on the hidden states of each of the model’s 32 transformer layers, while the pretrained model parameters remained frozen. Unless specified, inputs to the probes were derived from the model’s processing of prompts like ‘Calculate: num1 + num2 =’. General details on probe architecture (typically a linear

classification layer with Softmax) and training procedures (including standardized dataset splits and random seeds) are provided in Appendix B. Results from similar experiments on other models are detailed in Appendix D.

### 4.1 Formula structure representation

#### Arithmetic Structure Recognition Experiments:

To investigate the model’s ability to recognize arithmetic expression structures, we trained diagnostic probes to differentiate among three types of addition expressions involving two-digit positive integers (a+b, b+a, and a+a, where a>b). The dataset composition for this task is detailed in B.2. As shown in Fig. 2, the model demonstrated a strong ability to recognize the equation type, even in early layers. Notably, for the more challenging 4-digit generalization task, accuracy reached nearly 100% by layer 14.

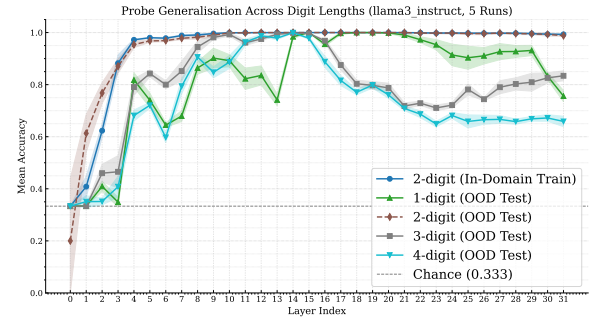


Figure 2: Probe trained on a two-digit addition dataset, accuracy of addition at different digits

### 4.2 Emergence of core computational features

**Arithmetic results Experiments:** We examined at which network layer the model can accurately predict the sum of addition problems. Probes were trained to classify problems based on their operational results, using densely distributed sum ranges (e.g., 500-509) to minimize chance predictions. Specifics of dataset generation, with 400 samples per sum class, are in C. As depicted in Figure 3, predictive accuracy for sums showed a consistent trend: near-baseline performance in shallow layers (0-8), a gradual increase from layer 8, a sharp rise around layer 16, and stabilization near 100% accuracy from layer 19 onwards.

**Carry signal experiment:** The model’s processing of carry mechanisms in three-digit addition was studied using probes trained to detect carries at the hundreds, tens, and units places. Three distinct



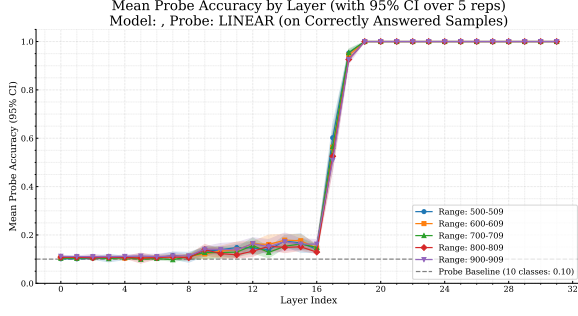


Figure 3: Comparison of the accuracy of each model layer on the arithmetic detection task for different numerical ranges (500-509 to 900-909). All tested ranges show a sharp rise in accuracy around layer 19.

datasets were created, each balanced for carry/no-carry instances at the specified decimal position (details in C.1). Figure 4 shows that probe accuracy for carry signals began a steady upward trend around layer 14, achieving near-100% accuracy for all decimal positions by layer 19, indicating efficient processing of carry information at this depth.

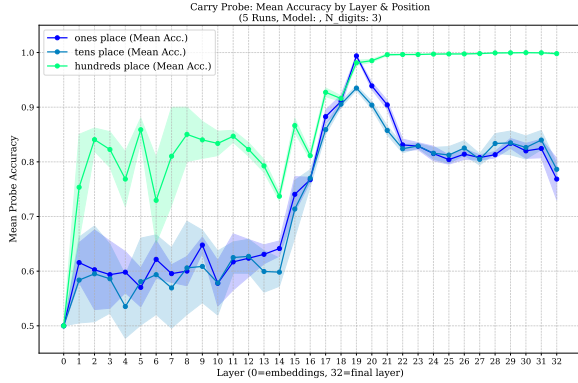


Figure 4: Carry operation detection: The recognition accuracy of the values of the ones, tens, and hundreds digits at each layer of the model, with 0.50 as the random baseline

### 4.3 Numerical abstraction of results

**Numerical abstraction Experiment:** This experiment investigated the emergence of numerical abstraction by probing at which network layer individual digits of a sum (constrained to three digits) are distinctly represented. The dataset construction is described in C.4. As depicted in Figure 5, the model’s ability to distinguish individual digits improved with network depth, starting from middle layers and reaching high, stable accuracy in deeper layers (e.g., after layer 28).

To assess generalizability, a probe trained to identify the hundreds digit in addition results

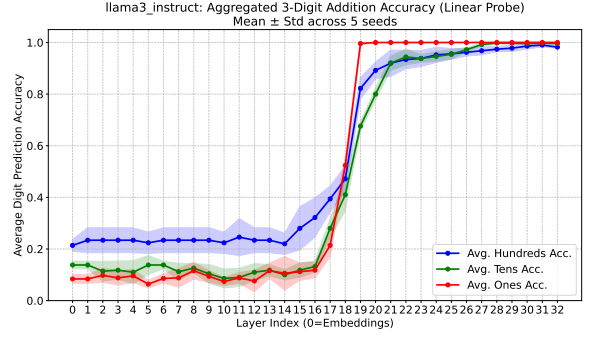


Figure 5: Compare the recognition accuracy of the model for the ones, tens, and hundreds of digits at each layer. The detection accuracy of each digit increases with the number of layers and tends to saturate at high accuracies in later layers (e.g., after the 28th layer), which is much higher than the random baseline of 0.10.

was tested on subtraction and multiplication tasks (dataset details in C.4). Figure 6 shows strong generalization to multiplication (peak accuracy >0.8) and moderate generalization to subtraction (peak accuracy 0.6-0.7). This suggests that while some numerical representations are shared, operation-specific features also play a role.

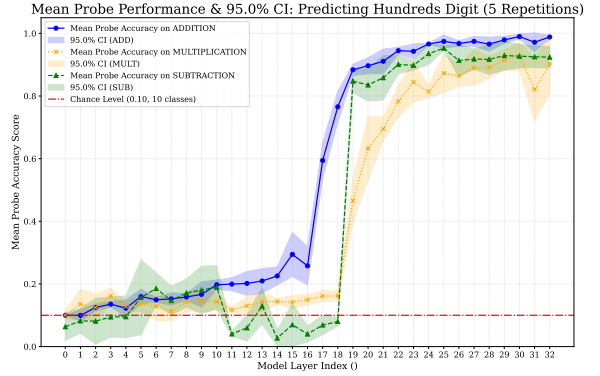


Figure 6: Comparison of the hundreds digit detection accuracy when applying a probe trained on an addition task to addition, multiplication, and subtraction test sets.

### 4.4 Logit-lens: Organization and generation of output content

**First-Correct-Token Emergence Experiment:** Using the Logit Lens technique, we identified the earliest layer at which the model explicitly encodes the correct sum token for addition problems involving two three-digit addends yielding a three-digit sum (dataset specifics in C.5). The analysis (Figure 7) revealed that initial top-1 predictions for all samples occurred late in processing, between layers 23 and 31, peaking at layer 30 (45.4% of

samples). This suggests that decisive arithmetic computation and answer finalization occur in the network’s concluding stages.

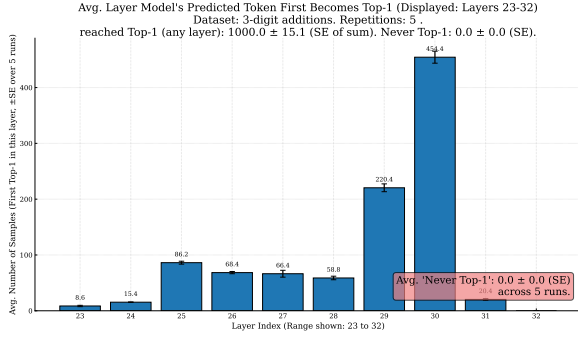


Figure 7: Logit Lens analysis of layers 23-32, showing the distribution of samples (N=1000) where the correct sum token was first identified as top-1. All initial identifications occurred in this range

## 5 Analysis

The experimental results of this study systematically reveal that when the LLaMA3-8B-Instruct large language model processes addition operations, the evolution of its internal information representation presents a clear, sequential trajectory.

Firstly, in the shallower layers of the network (e.g., in the formula structure recognition experiment, probes trained on two-digit numbers, when processing four-digit comparisons, show peak accuracy around layer 14), the model can efficiently identify the structural type of addition expressions (such as  $a+b$ ,  $b+a$ ,  $a+a$ ). At this point, the probe accuracy for decoding these structural features is high, especially its good generalization to different operand lengths, indicating that the model can capture the syntactic and basic semantic composition of the input arithmetic task at early computational depths.

Secondly, in the middle layers of the network (roughly from layer 14 to layer 18), the decodability of core arithmetic operation features begins to become prominent. The decoding accuracy for the representation of carry signals (whether for units, tens, or hundreds digits) significantly improves in this interval, reaching a near-perfect level around layer 19, forming a clear and easily decodable representation of the key steps of the operation. Almost simultaneously (starting with a sharp rise from layer 16 and stabilizing around layers 17-18), the prediction accuracy for the overall addition result (i.e., the "sum") also reaches saturation, sug-

gesting that a stable internal representation of the result is largely formed by these layers.

Subsequently, in the deeper layers of the network (especially after layer 25), probe results indicate that the model appears to focus more on a detailed numerical abstraction of the operation result. Experiments show that in these deeper layers, the model can accurately distinguish and represent the individual digits composing the "sum" (such as the hundreds digit, tens digit, units digit), linking the operation result with its specific numerical attributes. Logit Lens analysis further indicates that the generation of the final answer token primarily occurs in the final stages of the network (layers 23 to 31, peaking at layer 28). This is sequentially consistent with the maturation point of internal numerical representations (after layer 25), suggesting a potential transformation process within the model from internal numerical concepts to the final text output.

Furthermore, in the "arithmetic result experiment," the probe accuracy for sums across different numerical ranges (500-509 to 900-909) shows a highly consistent trend with increasing layer depth, all reaching high accuracy at similar levels (around layers 16-19). This indicates that, from the perspective of the evolution pattern of probe accuracy, these specific numerical range problems do not exhibit a significant difficulty gradient in terms of "when they become solvable" within the model’s internal processing.

## 6 Discussion

The sequential evolution pattern of information representation observed in this experiment provides important clues for understanding how LLMs perform arithmetic operations. Several phenomena are worth further discussion:

Firstly, **representations are dynamic**, with their prominence peaking at specific positions in the processing trajectory, sometimes followed by a slight decrease in decodability. This 'low-high-slight decrease' pattern was observed in several probe experiments. For instance, in the formula structure representation task (Fig. 2, focusing on probes trained on 2-digit addition), the accuracy for identifying '2-digit (In-Domain Train)' patterns peaks around layer 10 and then shows a gradual decline. Similarly, the '4-digit (OOD Test)' curve in the same figure peaks around layer 14 before decreasing. A similar trend is observable in the

carry signal experiment (Fig. 4). For example, the 'hundreds place' carry detection accuracy sharply peaks around layer 19-20, then exhibits a noticeable decrease in subsequent layers before a slight rebound. The 'tens place' and 'ones place' also show peaks (around layer 19 and 18 respectively) followed by a dip.

This pattern suggests that initially, accuracy is low as the specific arithmetic representation has not yet clearly formed. In intermediate layers, this information becomes most linearly decodable, and its representation strength and accessibility reach their peak. Subsequently, as the model processes this information or integrates it for subsequent computational stages, it may shift focus. Newly accumulated representational information from later layers (via residual connections) or the transformation of these features for downstream tasks might slightly interfere with or partially obscure the previously formed representations that are no longer central to the immediate next step of computation. This reflects the dynamic evolutionary nature of the model's internal representations, where specific information (as detected by our probes) is most clearly and accessibly represented at particular depths, rather than being monotonically refined.

**Secondly, Generalizability of representation.** Generalization experiments on the three-digit number recognition task show that a probe trained on addition generalizes very well to both subtraction and multiplication (each with accuracy approaching 90%), and that its generalization to subtraction is even stronger than to multiplication. The relatively superior generalization to subtraction (i.e., marginally better performance at similarly high levels) may indicate that in this model's representation learning, subtraction and addition share more direct or more readily transferable numerical representation elements. Although multiplication (conceptually a form of repeated addition, and likewise exhibiting good generalization here) also achieves a high degree of transfer, it falls slightly short of subtraction. This suggests that, despite substantial commonality, the computational mechanism the model learns for multiplication—or the representations it forms—retain some distinctive aspects that render its transfer a bit less effective than subtraction. Overall, this shows that the model's learned numerical representations combine a certain level of abstraction and cross-operation universality with features that are specific to each arithmetic operation.

Thirdly, **the analogical nature of the model's "computation" process.** The sequential emergence and progressive refinement of features revealed in this study bear resemblance to the cognitive processes humans use to solve arithmetic problems, which involve breaking down steps and calculating progressively. From identifying the structure of the expression, to processing carries, calculating the sum, and finally confirming and expressing each digit, the model internally appears to be executing a structured, computation-like process, rather than simple pattern matching or memory retrieval.

## 7 Conclusion

Through a series of carefully designed probe experiments on the LLaMA3-8B-Instruct model, and with comparative analyses on other representative models (detailed in Appendix D), this study systematically investigated their internal information processing mechanisms when performing addition operations. The main conclusions regarding LLaMA3-8B-Instruct are as follows:

### Sequential Information Processing Trajectory:

Our findings indicate that when LLaMA3-8B-Instruct processes addition operations, the decodability of its internal arithmetic features presents a coherent, sequential evolution pattern, outlining a multi-step information processing trajectory. Information at different levels, such as the recognition of formula structure, the emergence of features related to core operations (including carry and summation), and the numerical abstraction and output organization of the result, corresponds to representations that become clearly discernible at different, sequential depths of the network.

**Formation of Explicit Representations:** At various nodes of this processing trajectory (corresponding to different network depths), the model forms internal representations of specific arithmetic features (such as carries, sum values, individual digits) that are clear, stable, and easily decodable by linear probes, and the strength of these representations changes dynamically as processing proceeds.

### Support for "Computation-like" Process over "Rote Memorization":

The observed sequential emergence of features, the intrinsic connection between the operation results and their numerical attributes, the dynamic evolution of representations, and a certain degree of cross-task generalization

capability collectively constitute strong evidence. This suggests that when LLaMA3-8B-Instruct encounters simple addition problems within its training distribution, it is more inclined to perform a structured, "computation-like" process rather than primarily relying on large-scale pattern memorization.

Furthermore, comparative analyses with Mistral-7B-Instruct (see D for full details) revealed that the observed sequential processing trajectory and computation-like mechanisms are largely consistent across different model architectures, though with variations in the specific layers at which features emerge / certain model-specific strategies in representing numerical attributes which helps to contextualize the findings from LLaMA3-8B-Instruct and underscores the broader relevance of these information processing principles in LLMs.

In summary, the findings of this study deepen the understanding of the arithmetic capabilities of LLMs and provide empirical evidence for their complex internal information processing mechanisms, particularly revealing an ordered, computation-like internal information representation evolution path

## Limitations

Our study offers a first layer-wise picture of how LLaMA-3-8B-INSTRUCT handles multi-digit addition, but several caveats temper the strength of our claims.

**Correlation vs. causation.** The entire analysis relies on *correlational* tools—linear probes and the Logit Lens. These methods reveal that certain features *can* be linearly decoded from hidden states, but they do not prove that the forward pass *uses* those features, nor that the model follows an algorithmic carry-propagation procedure. To establish that the model truly *depends* on such internal computations (rather than exploiting spurious cues), future work will incorporate causal interventions such as activation patching, ablation, or circuit surgery

**Task scope.** We restrict attention to in-distribution, base-10 addition with short prompts of the form "Calculate:  $a+b =$  ". Borrowing subtraction, long multiplication, mixed-base arithmetic, or adversarial inputs remain unexplored; the four-stage trajectory we observe may not generalize to these settings.

**Model specificity.** Our observations are limited to two specific models, each tested with a corresponding checkpoint. Consequently, these findings cannot be generalized to suggest that all LLMs will exhibit the same representations. Factors such as different model architectures, sizes, tokenizer variants, or fine-tuned checkpoints would likely lead to different representational outcomes.

These limitations underscore the exploratory nature of our findings and motivate deeper, causally grounded circuit analyses across tasks, architectures, and arithmetic domains.

## Ethical Considerations

This research focuses on investigating the internal information processing pathways of Large Language Models (LLMs) when performing basic multi-digit addition. The core of the study involves analyzing internal model activations using techniques like linear probing and logit-lens to understand their computational mechanisms, rather than developing new applications or models.

We assess that this specific research work itself does not present significant ethical risks, for the following reasons:

1. **Benign Nature of the Task:** The problem under investigation (multi-digit addition) is a fundamental and well-defined arithmetic task that does not involve sensitive content, personal data, or socially charged issues that might introduce bias.
2. **Non-sensitive Data:** The datasets used in this study (e.g., prompts of the form "Calculate:  $\text{num1}+\text{num2} =$  " and corresponding arithmetic problems) are synthetically constructed for the research purpose and do not contain any personally identifiable information or other sensitive information.
3. **Transparency in Research Aim:** This study aims to enhance the understanding of the internal workings of LLMs, contributing to model interpretability and transparency.

While Large Language Models as a broader technology may raise various ethical considerations (such as bias, misuse, environmental impact, etc.), the scope of this research is limited to a mechanistic investigation of arithmetic capabilities in specific models (e.g., LLaMA-3-8B-Instruct). It does not directly engage with these broader ethical issues.



Therefore, we believe the direct ethical risks associated with the current work are minimal and manageable.

## References

- Yonatan Belinkov. 2022. [Probing classifiers: Promises, shortcomings, and advances](#). *Comput. Linguistics*, 48(1):207–219.
- Bilal Chughtai, Lawrence Chan, and Neel Nanda. 2023. [Neural networks learn representation theory: Reverse engineering how networks perform group operations](#). In *ICLR 2023 Workshop on Physics for Machine Learning*.
- Aaron Grattafiori, Abhimanyu Dubey, Abhinav Jauhri, Abhinav Pandey, Abhishek Kadian, Ahmad Al-Dahle, Aiesha Letman, Akhil Mathur, Alan Schelten, Alex Vaughan, and 1 others. 2024. The llama 3 herd of models. *arXiv preprint arXiv:2407.21783*.
- Yifan Hou, Jiaoda Li, Yu Fei, Alessandro Stolfo, Wangchunshu Zhou, Guangtao Zeng, Antoine Bosselut, and Mrinmaya Sachan. 2023. [Towards a mechanistic interpretation of multi-step reasoning capabilities of language models](#). In *Proceedings of the 2023 Conference on Empirical Methods in Natural Language Processing, EMNLP 2023, Singapore, December 6-10, 2023*, pages 4902–4919. Association for Computational Linguistics.
- Binyuan Hui, Jian Yang, Zeyu Cui, Jiaxi Yang, Dayiheng Liu, Lei Zhang, Tianyu Liu, Jiajun Zhang, Bowen Yu, Keming Lu, Kai Dang, Yang Fan, Yichang Zhang, An Yang, Rui Men, Fei Huang, Bo Zheng, Yibo Miao, Shanghaoran Quan, and 5 others. 2024. [Qwen2.5-coder technical report](#). *Preprint*, arXiv:2409.12186.
- Albert Q. Jiang, Alexandre Sablayrolles, Arthur Mensch, Chris Bamford, Devendra Singh Chaplot, Diego de las Casas, Florian Bressand, Gianna Lengyel, Guillaume Lample, Lucile Saulnier, L  lio Renard Lavaud, Marie-Anne Lachaux, Pierre Stock, Teven Le Scao, Thibaut Lavril, Thomas Wang, Timoth  e Lacroix, and William El Sayed. 2023. [Mistral 7b](#). *Preprint*, arXiv:2310.06825.
- Subhash Kantamneni and Max Tegmark. 2025. [Language models use trigonometry to do addition](#). In *ICLR 2025 Workshop on Building Trust in Language Models and Applications*.
- Jorrit Kruthoff. 2024. [Carrying over algorithm in transformers](#). *Preprint*, arXiv:2401.07993.
- Amit Arnold Levy and Mor Geva. 2025. [Language models encode numbers using digit representations in base 10](#). In *Proceedings of the 2025 Conference of the Nations of the Americas Chapter of the Association for Computational Linguistics: Human Language Technologies (Volume 2: Short Papers)*, pages 385–395, Albuquerque, New Mexico. Association for Computational Linguistics.
- Neel Nanda, Lawrence Chan, Tom Lieberum, Jess Smith, and Jacob Steinhardt. 2023. [Progress measures for grokking via mechanistic interpretability](#). In *The Eleventh International Conference on Learning Representations, ICLR 2023, Kigali, Rwanda, May 1-5, 2023*. OpenReview.net.
- Yaniv Nikankin, Anja Reusch, Aaron Mueller, and Yonatan Belinkov. 2024. [Arithmetic without algorithms: Language models solve math with a bag of heuristics](#). *Preprint*, arXiv:2410.21272.
- nostalgebraist. 2020. Interpreting gpt: the logit lens. <https://www.lesswrong.com/posts/AcKRB8wDpdaN6v6ru/interpreting-gpt-the-logit-lens>. LessWrong blog post.
- Philip Quirke and Fazl Barez. 2024. [Understanding addition in transformers](#). In *The Twelfth International Conference on Learning Representations, ICLR 2024, Vienna, Austria, May 7-11, 2024*. OpenReview.net.
- Alessandro Stolfo, Yonatan Belinkov, and Mrinmaya Sachan. 2023. [A mechanistic interpretation of arithmetic reasoning in language models using causal mediation analysis](#). In *Proceedings of the 2023 Conference on Empirical Methods in Natural Language Processing, EMNLP 2023, Singapore, December 6-10, 2023*, pages 7035–7052. Association for Computational Linguistics.
- Yang Yan, Yu Lu, Renjun Xu, and Zhenzhong Lan. 2025. [Do phd-level llms truly grasp elementary addition? probing rule learning vs. memorization in large language models](#). *Preprint*, arXiv:2504.05262.
- An Yang, Anfeng Li, Baosong Yang, Beichen Zhang, Binyuan Hui, Bo Zheng, Bowen Yu, Chang Gao, Chengen Huang, Chenxu Lv, Chuji   Zheng, Dayiheng Liu, Fan Zhou, Fei Huang, Feng Hu, Hao Ge, Haoran Wei, Huan Lin, Jialong Tang, and 41 others. 2025. [Qwen3 technical report](#). *Preprint*, arXiv:2505.09388.
- Zeping Yu and Sophia Ananiadou. 2024. [Interpreting arithmetic mechanism in large language models through comparative neuron analysis](#). In *Proceedings of the 2024 Conference on Empirical Methods in Natural Language Processing*, pages 3293–3306, Miami, Florida, USA. Association for Computational Linguistics.
- Tianyi Zhou, Deqing Fu, Vatsal Sharan, and Robin Jia. 2024. [Pre-trained large language models use fourier features to compute addition](#). In *Advances in Neural Information Processing Systems*, volume 37, pages 25120–25151. Curran Associates, Inc.
- Fangwei Zhu, Damai Dai, and Zhifang Sui. 2025. [Language models encode the value of numbers linearly](#). In *Proceedings of the 31st International Conference on Computational Linguistics, COLING 2025, Abu Dhabi, UAE, January 19-24, 2025*, pages 693–709. Association for Computational Linguistics.

## A Detailed Model Performance Metrics

This appendix presents a detailed summary of the performance metrics for the different language models evaluated in this study. Table 2 offers a comparative analysis of these models based on their accuracy in specific numerical prediction tasks.

Each row in the table corresponds to a distinct language model, identified under the "Model ID" column. The "Overall Accuracy" column provides a general measure of each model's performance across all evaluated tasks. The subsequent columns, labeled from "1-digit" through "6-digit," specify the model's accuracy in correctly predicting numerical values composed of one to six digits, respectively. All accuracy figures presented in the table are expressed as percentages. This data provides insight into the capabilities and limitations of each model concerning tasks that require numerical precision and understanding of magnitude.

## B General Experimental Setup

### B.1 Language Model

All experiments used the LLaMA3-8B-Instruct model. Model parameters were kept frozen for all probing runs. The network has 32 transformer layers.

### B.2 Input Representation for Probes

For each of the 32 layers an independent diagnostic probe was trained. The probe input was the hidden state of the *last* token of the prompt Calculate: num1 + num2 =—namely the trailing space after the "=" sign.

### B.3 Probe Architecture

Unless otherwise stated (see [Appendix C](#)), every probe consisted of

- a single linear classification layer, followed by
- a SOFTMAX activation.

This yields a probability distribution over the task-specific classes.

### B.4 Training and Evaluation

- **Data splitting:** Each dataset was split 80%/20% into train/test using stratified sampling to preserve class ratios.

- **Replications:** All experiments were run five times with random seeds 42–46; reported scores are the mean over runs.

## C Experiment-Specific Details

### C.1 Formula Structure Representation (Addition-Order Experiments)

**Task.** Distinguish three expression types for two-digit integers  $a, b \in [10, 99]$  with  $a > b$ :

1.  $a + b$  (e.g.  $45 + 23$ )
2.  $b + a$  (e.g.  $23 + 45$ )
3.  $a + a$  (e.g.  $66 + 66$ )

**Training data.**

- Type 1: 5000 random samples
- Type 2: 5000 random samples
- Type 3: 80% of the 90 unique pairs

**Generalization tests.** Three extra test sets mirror the above but use one-, three-, and four-digit addends, respectively.

### C.2 Emergence of Core Computational Features (Arithmetic-Results Experiments)

**Task.** Predict the exact sum; each class is one sum value.

**Dataset generation.**

- 400 examples per class with unconstrained addends.
- Five groups of sums: 500–509, 600–609, 700–709, 800–809, 900–909.

### C.3 Carry-Signal Experiment

**Task.** Binary classification—detect a carry in the units, tens, or hundreds place of three-digit additions.

**Datasets.** Three balanced sets of 1 000 problems each (one per decimal place). A single problem may appear in several sets if its carries differ by place.

### C.4 Numerical Abstraction of Results

**Digit-identification task.** Given a sum that is three digits long, predict its hundreds, tens, and units digits (10-way classification each). The dataset contains 1 000 two-addend problems.

Model ID	Overall Accuracy	1-digit	2-digit	3-digit	4-digit	5-digit	6-digit
Llama3-8B-Instruct	97.29%	100.00%	100.00%	99.70%	95.51%	93.21%	95.31%
Mistral-7B-Instruct-v0.2	84.99%	98.81%	83.05%	89.03%	84.63%	79.94%	74.45%
Qwen3-8B	63.98%	92.18%	79.52%	52.09%	57.57%	54.00%	48.53%
Qwen2.5-7B-Instruct	60.61%	77.31%	71.88%	67.90%	37.03%	50.50%	58.98%

Table 2: Overall Model Performance Summary. This table shows the accuracy of different models across various digit prediction tasks. The target for each group was to collect 4000 samples, though some groups had fewer (for example, the 1-digit group only contained 55 samples).

**Hundreds-digit generalization.** A probe trained on hundreds-digit identification was also tested on subtraction and multiplication datasets whose results are mostly three-digit numbers, generated with the same principles.

## C.5 Logit-Lens Analysis

**Task.** Find the earliest transformer layer whose output distribution ranks the correct sum token at top-1 (logit lens).

**Dataset.** 1000 randomly generated problems: two three-digit addends yielding a three-digit sum.

## D Mistral-7B-Instruct

### D.1 Mistral:Arithmetic Structure Recognition Experiments

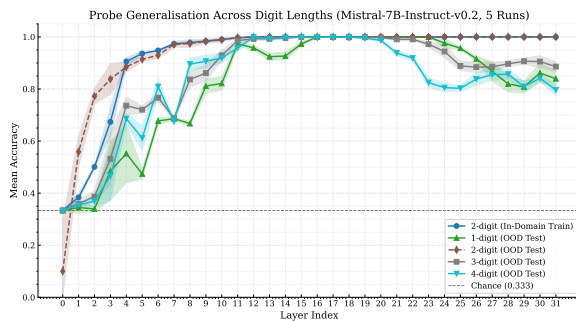


Figure 8: Probe trained on a two-digit addition dataset, accuracy of addition at different digits

### D.2 Mistral:Arithmetic results Experiments

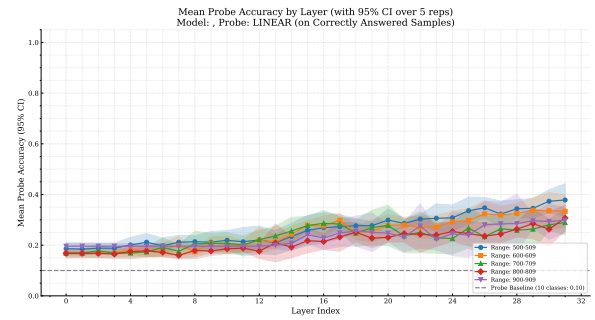


Figure 9: This chart compares the accuracy of each model layer on the arithmetic detection task for different numerical ranges (500-509 to 900-909). It should be noted that an experimental anomaly was observed: For instance, for the constructed dataset ' $a+b = 500$ ', correct samples constituted only about 10% of the total constructed samples, thus preventing the normal display of results for this section.

#### D.2.1 Mistral:Carry signal experiment

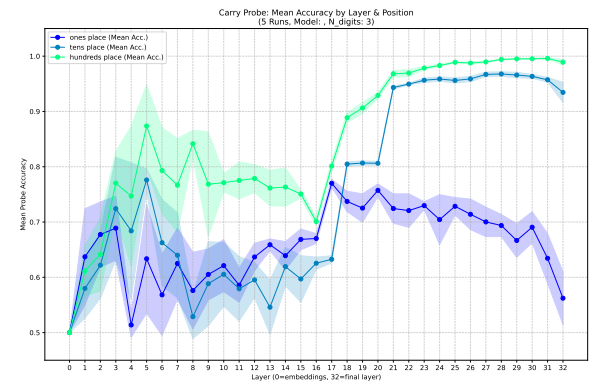


Figure 10: Carry operation detection: The recognition accuracy of the values of the ones, tens, and hundreds digits at each layer of the model

### D.3 Mistral:Determining Digits of Addition Results Experiment

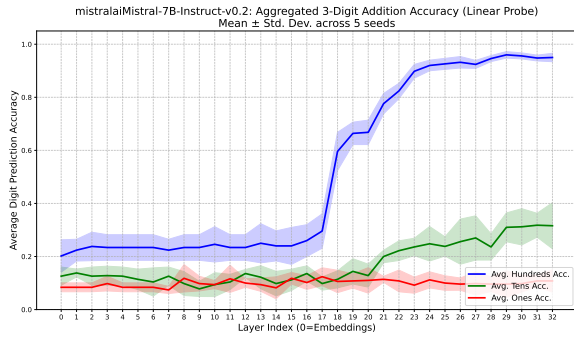


Figure 11: Compare the recognition accuracy of the model for the ones, tens, and hundreds of digits at each layer.

### D.4 Mistral:Numerical abstraction Experiment

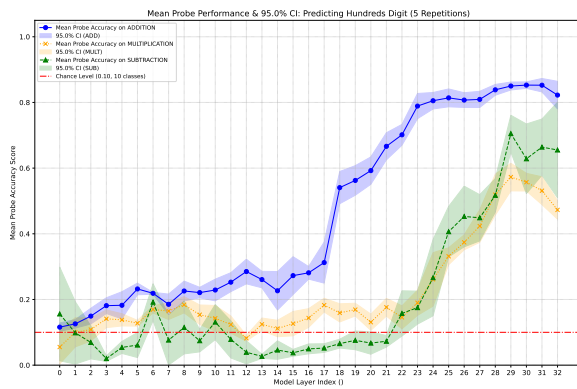


Figure 12: Comparison of the hundreds digit detection accuracy when applying a probe trained on an addition task to addition, multiplication, and subtraction test sets.

### D.5 Mistral:First-Correct-Token Emergence Experiment

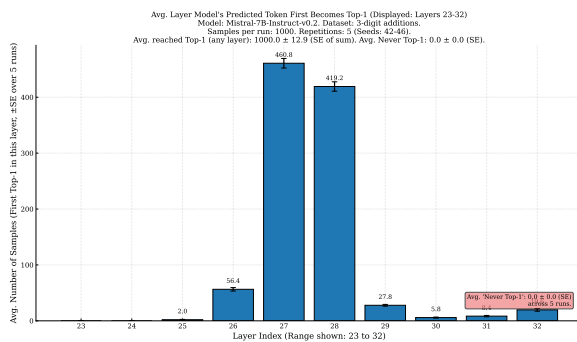


Figure 13: Logit Lens analysis of layers 23-32, showing the distribution of samples (N=1000) where the correct sum token was first identified as top-1.